Quadratic solitons for negative effective second-harmonic diffraction as nonlocal solitons with periodic nonlocal response function

B. K. Esbensen,[1] M. Bache,[1] W. Krolikowski,[2] and O. Bang[1]

[1]*DTU Fotonik, Department of Photonics Engineering, Technical University of Denmark, DK-2800 Kongens Lyngby, Denmark*

[2]*Laser Physics Centre, Research School of Physics and Engineering, Australian National University, Canberra, Australian Capital Territory 0200, Australia*

(Received 2 April 2012; published 28 August 2012)

We employ the formal analogy between quadratic and nonlocal solitons to investigate analytically the properties of solitons and soliton bound states in second-harmonic generation in the regime of negative diffraction or dispersion of the second harmonic. We show that in the nonlocal description this regime corresponds to a periodic nonlocal response function. We then use the strongly nonlocal approximation to find analytical solutions of the families of single bright solitons and their bound states in terms of Mathieu functions.

DOI: 10.1103/PhysRevA.86.023849 PACS number(s): 42.65.Tg, 42.65.Sf, 42.70.Df, 03.75.Lm

I. INTRODUCTION

Quadratic nonlinear or $\chi^{(2)}$ materials have a strong and fast electronic nonlinearity, which makes them excellent materials for the study of nonlinear effects, such as solitons [1]. The main properties of quadratic solitons are well known and both $(1+1)$-dimensional and $(2+1)$-dimensional bright spatial solitons have been observed experimentally [2]. The applicability of quadratic media, in particular in terms of second-harmonic (SH) generation, is further enhanced by the now mature quasi-phase-matching (QPM) technology, by which artificial phase matching can be achieved, in principle, in most $\chi^{(2)}$ crystals [3]. Such QPM gratings induce interesting switching properties [4,5] but still allows quadratic soliton solutions to exist [6,7], even when the QPM grating has a two-period or quasiperiodic domain length [8,9].

There has been significant interest in finding exact analytical formulas for families of quadratic soliton solutions. However, due to the nonintegrability of the governing model, this has not been possible. To understand the origin of the problem we need to consider the particular soliton model. After an appropriate scaling the simplest possible model for the transverse soliton profile of the fundamental wave ϕ_1 and the SH ϕ_2 has the form [10]

$$s_1\frac{\partial^2\phi_1}{\partial\tau^2}-\phi_1+\phi_1\phi_2=0, \tag{1}$$

$$s_2\frac{\partial^2\phi_2}{\partial\tau^2}-\alpha\phi_2+\frac{1}{2}\phi_1^2=0. \tag{2}$$

This equation has only one free parameter, α, in addition to the two sign parameters, $s_{1,2}=\pm1$. The transverse coordinate τ can represent either a spatial or a temporal coordinate, in which case the second derivative represents diffraction or dispersion, respectively.

A family of bright quadratic solitons has been found numerically for $s_1=s_2=+1$ and $\alpha>0$ [10], but only in the particular case of $\alpha=1$ does an exact analytical solution exist [11]. Similarly, for $s_1=-s_2=-1$ and $\alpha>0$, a family of dark quadratic soliton solutions can be found numerically [10]. Families of quadratic soliton solutions thus exists for $s_2=+1$, corresponding to positive diffraction and dispersion at the SH.

In the so-called cascading limit of $\alpha\gg1$ these solitons may be described as conventional bright and dark soliton solutions of the nonlinear Schrödinger (NLS) equation. This is not so when $s_2=-1$, in which case it has been shown that localized solutions of the cascading NLS limit will radiate linear waves due to parametric coupling with the SH [10]. In fact it was shown numerically by Buryak and Kivshar that for a discrete set of values of α, such radiative solitary waves could be combined in pairs to cancel out the oscillating tails outside the localization region and form stationary soliton solutions consisting of pairs of bright or dark solitons [10]. Because early studies showed that the solitons for $s_2=-1$ were unstable, all analytical studies have focused on the case when $s_2=+1$, where both variational calculations [12] and scaling transformations [13] have been used to find approximative analytical solutions.

The quadratic or parametric nonlinearity is not associated with an intensity-dependent refractive index as the Kerr nonlinearity is. Consequently, it is not so easy to use simple intuitive arguments to explain the properties of solitons using, e.g., concepts from waveguide theory. The NLS equation obtained in the cascading limit $|\alpha|\gg1$ fails in many aspects, because it "slaves" the SH to the fundamental, both dynamically and spatially, by the approximation $\phi_2=\phi_1^2/(2\alpha)$. Thus it predicts the existence of collapse, which is known not to occur in quadratic nonlinear materials [14], and it cannot predict any dependence on s_2. A simple phase-shift approach was proposed by Assanto and Stegeman [15] which could explain several soliton related effects. However, it predicts, e.g., that two dark solitons and two out-of-phase bright solitons will always repel and thus can never form a bound state, whereas it is known that such bound states of quadratic solitons do exist [10].

In 2002 Shadrivov and Zharov, in a study of quadratic nonlinear interface waves, noted that for s_1, s_2, and α all positive, Eqs. (1) and (2) could be solved formally using a nonlocal response function, $\phi_2(\tau)=\frac{1}{4\sqrt{\alpha}}\int_{-\infty}^{\infty}\phi_1^2(\tau')\exp(-\sqrt{\alpha}|\tau'-\tau|)d\tau'$, just as for general nonlocal media [16]. They then used what is known as the strongly nonlocal limit, $\alpha\ll1$, to obtain a linear model that could be solved analytically to find a family of multihump bright solitons [17]. This formal equivalence of

stationary bright solitons in nonlocal media and parametric solitons was also discussed by Conti *et al*. in 2003 in a study of liquid crystals [18].

A further step forward in the understanding of quadratic solitons was made in 2003, when a *dynamical phase-sensitive* nonlocal model was proposed by Nikolov *et al*. based on the analogy between parametric interaction and diffusive nonlocality [19]. The nonlocal theory is physically intuitive, it is exact in predicting the profiles of stationary quadratic solitons, and it provides a simple physical explanation for their properties. In this later work the nonlocal theory was shown to give a broad physical picture in the whole regime of existence of solitons, and it was used to discuss the until then unresolved problem of dark solitons and bound states of out-of-phase bright solitons [19]. Evidently, the nonlocal analogy also explains the absence of collapse in the $\chi^{(2)}$ model as being due to nonlocality, which is known to completely arrest collapse [20,21], in contrast to, for example, incoherence [22,23] or noise [24], which merely delays it.

The nonlocal analogy has now been used to successfully describe pulse compression [25,26], the formation of $(2+1)$-dimensional X waves [27], and modulational instability [28] in quadratic nonlinear materials. Here we use the analogy to study the hitherto untractable regime for quadratic solitons, where $s_2 = -1$. This case was not treated by Shadrivov and Zharov [17] or Conti *et al*. [18], but it was briefly discussed by Nikolov *et al*., who derived the corresponding response function and showed that it was not localized as for $s_2 = +1$, but was oscillatory [19]. Nikolov *et al*. conjectured that this oscillatory response function explains the fact that dark and bright quadratic solitons radiate linear waves for $s_2 = -1$, as was originally found by Buryak and Kivshar [10].

Here we analytically consider $\chi^{(2)}$ materials for $s_2 = -1$ in more detail. We derive the nonlocal response function and show that in this regime it is periodic and thus importantly cannot be normalized. We show that in the strongly nonlocal regime, the model reduces to Mathieu's differential equation [29], which has both periodic and aperiodic solutions. We use the exact solutions to construct families of single-soliton and soliton bound-state solutions, which are exact analytical solutions in the strongly nonlocal limit. Finally, we study the solutions numerically by propagating them in the original $\chi^{(2)}$ model in order to demonstrate for how long they can remain stationary before their known instability sets in.

II. NONLOCAL MODEL FOR QUADRATIC SOLITONS

We consider a fundamental wave (FW) and its SH propagating along the z direction in a lossless quadratic nonlinear medium under conditions for type-I phase matching. The normalized dynamical equations for the slowly varying envelopes $E_{1,2}(x,z)$ are then [30,31]

$$i\frac{\partial E_1}{\partial z} + \gamma_1\frac{\partial^2 E_1}{\partial x^2} + \chi_1 E_1^* E_2 e^{-i\Delta k z} = 0, \tag{3}$$

$$i\frac{\partial E_2}{\partial z} + \gamma_2\frac{\partial^2 E_2}{\partial x^2} + \chi_2 E_1^2 e^{i\Delta k z} = 0, \tag{4}$$

where $\chi_1 = 4\pi\omega^2\chi^{(2)}(-\omega;2\omega,-\omega)/(k_1c^2)$ and $\chi_2 = 8\pi\omega^2\chi^{(2)}(-2\omega;\omega,\omega)/(k_2c^2)$, z is the propagation distance, and $\Delta k = k_2 - 2k_1$ is the wave-vector mismatch. x is the transverse coordinate, and $\gamma_j = 1/(2k_j)$ $(j = 1,2)$, so the effect of diffraction is taken into account. We note that the second derivative term also can represent dispersion, but here and in the following we denote it as diffraction [31]. In the spatial domain $\gamma_1 \approx 2\gamma_2$ and $\gamma_j > 0$. Applying the exact transformations,

$$E_1 = w\frac{1}{\eta\sqrt{\chi_1\chi_2}}, \quad E_2 = v\frac{1}{\eta\chi_1},$$

where η is a characteristic length, the equations for w and v take the form

$$i\frac{\partial w}{\partial\zeta} + d_1\frac{\partial^2 w}{\partial\xi^2} + w^* v e^{-i\beta\zeta} = 0, \tag{5}$$

$$i\frac{\partial v}{\partial\zeta} + d_2\frac{\partial^2 v}{\partial\xi^2} + w^2 e^{i\beta\zeta} = 0, \tag{6}$$

where $\beta = \Delta k\eta$ is the normalized wave-vector mismatch, $\zeta = z/\eta$, $\xi = x/\eta$, and $d_j = \gamma_j/\eta$.

In the cascading limit the phase mismatch is large, $\beta^{-1} \to 0$, and the nonlocal approach takes the ansatz $v = \bar{v}e^{i\beta\zeta}$. Assuming slow variation of $\bar{v}$ in both the propagation and transverse directions gives the NLS equation [19],

$$i\frac{\partial w}{\partial\zeta} + d_1\frac{\partial^2 w}{\partial\xi^2} + \beta^{-1}|w|^2 w = 0, \tag{7}$$

in which the local Kerr nonlinearity is due to the coupling to the SH field $\bar{v} = \beta^{-1}w^2$. In this case the SH is slaved to the FW, and the width of both is fixed. The NLS equation is inaccurate even for stationary solutions because the term $\partial^2 v/\partial\xi^2$ in Eq. (6) is neglected. To obtain a more accurate *dynamical model* than that given by the cascading limit, slow variation of $\bar{v}$ could be assumed *only in the propagation direction*, i.e., neglecting only the $\partial v/\partial\zeta$ term [19].

However, here we focus on stationary solutions to Eqs. (5) and (6) of the form

$$w = a_1\phi_1(\tau)e^{i\lambda\zeta}, \quad v = a_2\phi_2(\tau)e^{2i\lambda\zeta + i\beta\zeta},$$

where the profiles ϕ_j are real, λ is a solution parameter, $\tau = \xi\sqrt{|\lambda/d_1|}$, $a_1^2 = \lambda^2|d_2/(2d_1)|$, and $a_2 = \lambda$. This scaling reduces the number of free parameters to one [10] and transforms Eqs. (5) and (6) into Eqs. (1) and (2), with $s_j = \mathrm{sgn}(\lambda d_j)$ and $\alpha = |d_1/d_2|(\beta + 2\lambda)/\lambda$. The properties of solitons described by Eqs. (1) and (2) are well known [10] with, e.g., a family of bright (dark) solitons existing for $s_1 = s_2 = +1$ $(-s_1 = s_2 = +1)$ and $\alpha > 0$, as also discussed in the Introduction.

Equation (2) can be solved exactly using Fourier transformation and the convolution theorem, treating ϕ_1^2 as a function. The relation between the SH and the FW then acquires the form of a convolution, leading to the exact nonlocal equation for the FW [19]:

$$s_1\frac{\partial^2\phi_1}{\partial\tau^2} - \phi_1 + \gamma\phi_1\int_{-\infty}^{\infty}\phi_1^2(s)Q(\tau - s)ds = 0, \tag{8}$$

where $\gamma = s_2\sigma^2/2$ and $s_3 = \mathrm{sgn}\{s_2\alpha\}$. In the Fourier k domain (denoted by a tilde) the response function is given by a Lorentzian,

$$\tilde{Q}(k) = \int_{-\infty}^{\infty} Q(\tau)e^{ik\tau}d\tau = \frac{1}{\sigma^2k^2 + s_3},$$

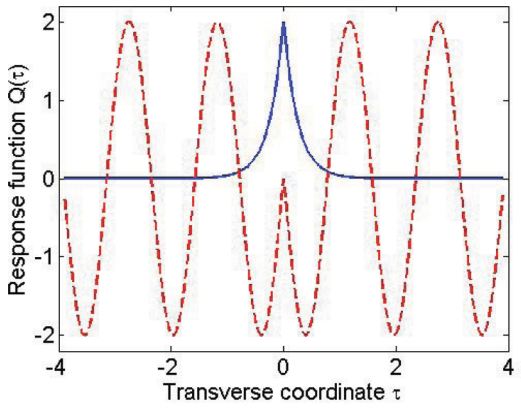

FIG. 1. (Color online) Localized response function $Q(\tau) = \frac{1}{2\sigma} e^{-|\tau|/\sigma}$ (solid blue line) for $s_3 = +1$. Oscillatory response function $Q(\tau) = -\frac{1}{2\sigma} \sin(|\tau|/\sigma)$ (dashed red line) for $s_3 = -1$. Here $\sigma = 0.25$.

where $\sigma = 1/\sqrt{|\alpha|}$. Equation (8) shows that the nonlinear coupling between the FW and the SH components of a $\chi^{(2)}$ soliton is identical to the FW experiencing a nonlocal Kerr nonlinearity. However, very importantly, the sign of the nonlinearity and the profile of the response function depend on the sign of the phase mismatch α and the sign of the SH diffraction s_2 through the parameters γ and s_3.

For $s_3 = +1$ the response function is given by $Q(\tau) = \frac{1}{2\sigma} e^{-|\tau|/\sigma}$, from which we recognize σ as the degree of nonlocality, i.e., the width of the response function. In this case, which physically resembles diffusion, the $\chi^{(2)}$ response function is localized and normalized, $\int_{-\infty}^{\infty} Q(\tau) d\tau = 1$. This means that the response function $Q(\tau)$ approaches a $\delta(\tau)$ function as the degree of nonlocality σ goes to zero and thus that one recaptures the cubic (Kerr) nonlinearity of the cascading limit.

For $s_3 = -1$ the Fourier transform of the response function has poles on the real k axis. In this case the response function becomes oscillatory, $Q(\tau) = -\frac{1}{2\sigma} \sin(|\tau|/\sigma)$, and therefore cannot be normalized. Physically, this means that the local limit of σ going to zero is unknown: it does not correspond to the simple cubic nonlinearity found in the cascading limit for $s_3 = +1$. The two different kinds of response functions are shown in Fig. 1.

A. Simple weakly nonlocal model: Exact solutions

Having established the nonlocal model for quadratic solitons, two important limits exists, in which the model can be simplified such as to lend itself to finding analytical solutions. If we consider the case $s_3 = +1$, where the $\chi^{(2)}$ response function is localized and normalized, then there exists the so-called weakly nonlocal limit, in which $\sigma \ll 1$ ($|\alpha| \gg 1$), and the response function $Q(\tau)$ is much narrower than the FW intensity $\phi_1^2(\tau)$. Taylor expanding $\phi_1^2(s)$ to second order around $s = \tau$ in the integral in Eq. (8) and using that the response function is symmetric then give the more simple, weakly nonlocal model:

$$s_1 \frac{\partial^2 \phi_1}{\partial \tau^2} - \phi_1 + \gamma \left(q_0 \phi_1^2 + q_2 \frac{\partial^2 \phi_1^2}{\partial \tau^2} \right) \phi_1 = 0, \tag{9}$$

where $q_0 = \int Q(z) dz = 1$ and $q_2 = \frac{1}{2} \int z^2 Q(z) dz = \sigma^2$ ($q_1 = 0$ due to symmetry). This model has exact bright soliton solutions for $s_1 = s_2 = +1$ and $\alpha > 0$ and exact dark soliton solutions for $-s_1 = s_2 = +1$ [19,32]. Unfortunately, due to the periodic nature of the $\chi^{(2)}$ response function for $s_3 = -1$, no simplified weakly nonlocal model exists in this case (the integrals q_0 and q_2 do not exist), which means that we have no simple way to find analytical solutions in this limit.

B. Simple strongly nonlocal model: Exact solutions

For $\sigma \gg 1$ ($|\alpha| \ll 1$) the nonlocality is strong. In the regime of a localized response function ($s_3 = +1$) the intensity profile of the FW is much narrower than the response function, and thus one can Taylor expand the response function $Q(\tau)$ under the integral in Eq. (8). For bright solitons, this means that to a good approximation one can take the response function outside the integral in Eq. (8) and arrive at the linear eigenvalue equation:

$$s_1 \frac{\partial^2 \phi_1}{\partial \tau^2} - \phi_1 + \frac{\gamma P_1}{2\sigma} \exp\left(\frac{|\tau|}{\sigma} \right) \phi_1 = 0, \tag{10}$$

where the FW power $P_1 = \int_{-\infty}^{\infty} \phi_1^2(s) ds$ has the role of the eigenvalue. This equation is known from linear waveguide theory and has exact solutions in the form of Bessel's function of the first kind [33], which was used in [17,19] to find families of single- and multihump bright solitons in the form of bound states of in-phase or out-of-phase single bright solitons. By taking special care of the dark soliton background in the expansion, this approach can also be used to find exact dark soliton solutions and their bound states [19].

All these bright and dark soliton solutions found by using the nonlocal analogy and taking the limit of strong nonlocality were shown to provide accurate predictions of the actual solutions, hitherto only demonstrated numerically [10]. This illustrates the strength of the nonlocal analogy in providing analytical treatment and physical insight into the properties of $\chi^{(2)}$ solitons.

Considering now the strongly nonlocal limit $\sigma \gg 1$ ($|\alpha| \ll 1$) for the case when $s_3 = -1$ and the response function is oscillatory, we again use the approach of taking the response function outside the integral in Eq. (8). Focusing solely on bright solitons, we then arrive at the linear equation,

$$s_1 \frac{\partial^2 \phi_1}{\partial \tau^2} - \phi_1 - \frac{\gamma P_1}{2\sigma} \sin\left(\frac{|\tau|}{\sigma} \right) \phi_1 = 0, \tag{11}$$

which is again a linear eigenvalue equation for the FW, in which the power of the FW, P_1, plays the role of the eigenvalue. The rest of this paper is concerned with solving Eq. (11), which also allows exact analytical solutions.

III. BRIGHT SOLITON SOLUTIONS FOR PERIODIC RESPONSE

If we consider $\tau \geqslant 0$ and make the substitution $\phi_1(\tau) = \mathrm{Re}\{\Phi(y)\}$, where $y = \tau/(2\sigma) - \pi/4$, then we transform Eq. (11) into

$$\frac{\partial^2 \Phi}{\partial y^2} + [a - 2q \cos(2y)] \Phi = 0, \tag{12}$$

where $a = -4s_1\sigma^2$ and $q = s_1 s_2 \sigma^3 P_1/2$ are real parameters, whereas the solution $\Phi(y)$ is allowed to be complex. When $\tau < 0$, we have an equation equivalent to Eq. (12) but with $q = -s_1 s_2 \sigma^3 P_1/2$. In particular this means that changing the sign of s_2 corresponds simply to a reflection $\tau \to -\tau$. If we look at the SH given by $\phi_2(\tau) = -\frac{1}{4} s_2 \sigma P_1 \sin(|\tau|/\sigma)$ and keep in mind that $s_3 = \mathrm{sgn}(s_2\alpha) = -1$ is fixed, then changing the sign of s_2 will change the sign of both ϕ_2 and α. This corresponds to the properties of the original Eq. (2), which is invariant to the scaling $(\phi_2, s_2, \alpha) \to (-\phi_2, -s_2, -\alpha)$. In particular, this means that without loss of generality we can fix $s_2 = -1$. We further restrict ourselves to the case of bright solitons, which means that $s_1 = +1$, and thus both parameters $a = -4\sigma^2$ and $q = -\sigma^3 P_1/2$ are negative.

Equation (12) is known as Mathieu's differential equation (MDE) [29], which arises, for example, in the description of wave propagation in periodic media, such as a particle in a Paul trap [34], cold atoms in an optical lattice [35], or optical beams in a medium with a periodic refractive index distribution [36]. The periodicity leads to the appearance of linear bands of allowed states of waves separated by forbidden gaps. However, the presence of defects in the periodicity allows the existence of so-called defect modes, i.e., spatially finite waves localized within the forbidden gaps [37]. This is exactly the situation we are dealing with here. The periodicity of the potential function in Eq. (11) is broken in $\tau = 0$, which enables soliton solutions to exist in the form of spatially localized states centered at $\tau = 0$.

In order to find soliton solutions we use the known properties of MDE and its solutions. Since the coefficients of MDE are periodic functions of y, it follows from the Floquet's theorem that for fixed values of (a,q), MDE admits a complex valued solution of the form [29]

$$F_\nu(a,q,y) = e^{i\nu y} P(a,q,y), \tag{13}$$

where $\nu = \nu(a,q)$ is a complex number that depends on a and q and $P(a,q,y)$ is a complex periodic function of the same period as that of the coefficients in MDE, namely, π. However, P is, in general, not sinusoidal. The constant ν is called the characteristic exponent. When $F_\nu(a,q,y)$ is a solution to MDE, then $F_\nu(a,q,-y) = e^{-i\nu y} P(a,q,-y)$ is also a solution. Both solutions have the property $F_\nu(\pm[y + k\pi]) = C^k F_\nu(\pm y)$, where $C = e^{\pm i\nu\pi}$ and k is an integer. Here a and q have been left out of the argument for convenience.

It can be shown that if parameter a in MDE belongs to a discrete set of characteristic bands $a_{\mathrm{even}}(q)$ and $a_{\mathrm{odd}}(q)$ (see Fig. 2), then ν is zero or an integer, resulting in even and odd strictly periodic solutions, respectively [29]. In fact, when ν is an integer $F_\nu(y)$ is proportional to $F_\nu(-y)$, and so a second independent solution to MDE is needed to span the complete solution space. However, we are here interested in spatially localized solutions, or defect modes, which exist for values of a and q in between the bands $a_{\mathrm{even}}(q)$ and $a_{\mathrm{odd}}(q)$, where ν is complex (see Fig. 2). This means that the two Floquet solutions $F_\nu(y)$ and $F_\nu(-y)$ are linearly independent, and the full solution to MDE is

$$\Phi(y) = c_1 F_\nu(a,q,y) + c_2 F_\nu(a,q,-y), \tag{14}$$

where c_1 and c_2 are constants. In the present case a and q are real, and ν can be real or complex, depending on which

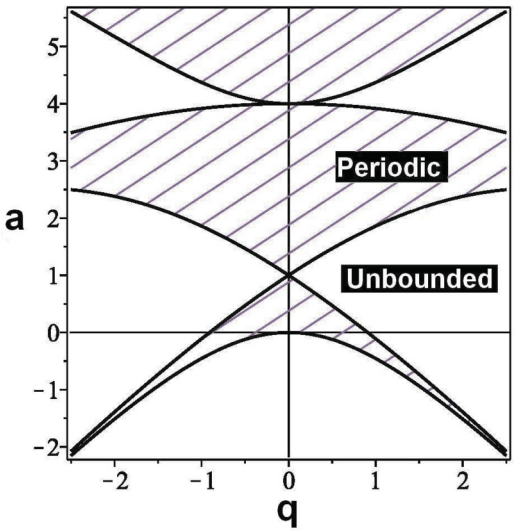

FIG. 2. Characteristic bands (black curves) of 2π periodic solutions to MDE, for which ν is an integer. In the shaded regions ν is real and the solutions are periodic. In the white regions ν is complex and the solutions become unbounded.

bands the values of a and q lie in between. If ν is real, all solutions to MDE are periodic and bounded. Here we consider only complex values of ν, for which every solution becomes infinite at least once in the whole y plane. The band structure in the (a,q) plane is shown in Fig. 2. In our case a and q are both negative, and thus we see from Fig. 2 that ν is complex in most of the region, separated by narrow bands of localized solutions. This is further detailed in Fig. 3, where we consider a typical situation and fix $\sigma = 1$, so that $a = -4$ and $q = -P_1/2$. As P_1 is increased from zero (q decreased from zero), we clearly see the appearance of narrow bands

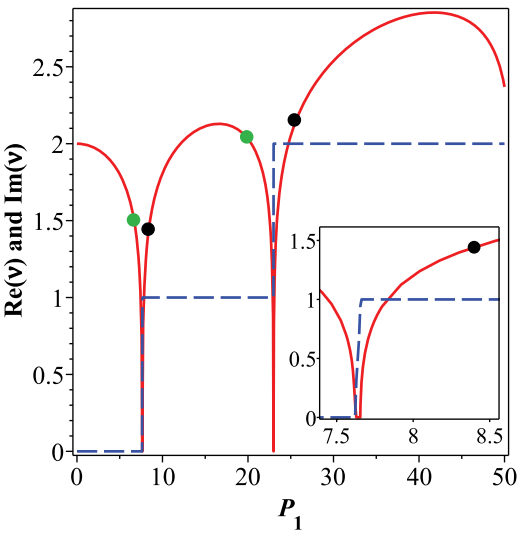

FIG. 3. (Color online) Real (dashed blue line) and imaginary (solid red line) parts of characteristic exponent ν for $\sigma = 1$ vs FW power P_1. Black dots mark the two lowest-power antisymmetric solutions with $P_1 = 8.40$ and 25.50 ($\nu = 1 + i1.44$ and $2 + i2.15$). Green dots mark the two lowest-power symmetric solutions with $P_1 = 6.69$ and 19.93 ($\nu = 0 + i1.50$ and $1 + i2.04$).

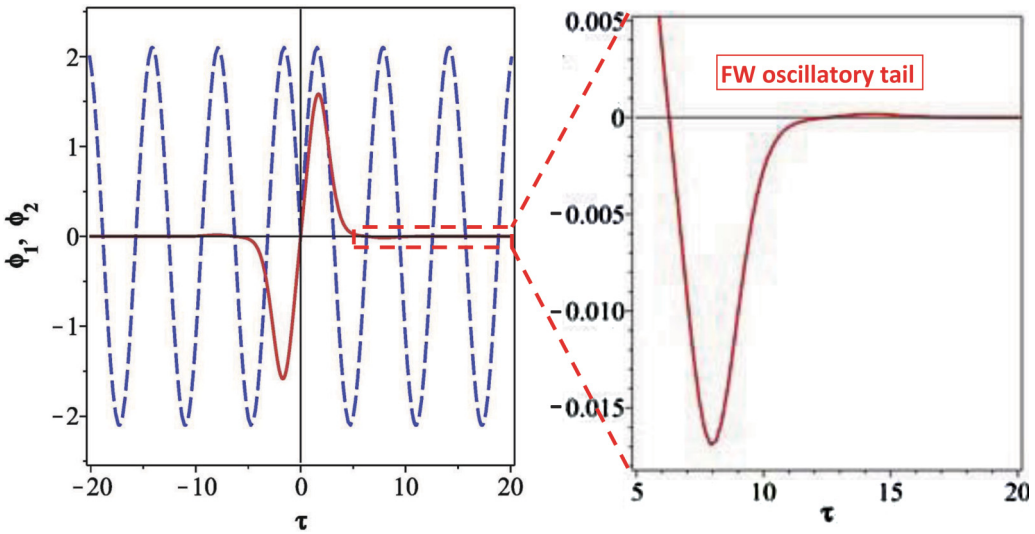

FIG. 4. (Color online) Antisymmetric solution with lowest power $P_1 = 8.40$ ($\nu = 1 + i\,1.44$) for $\sigma = 1$, showing both the FW $\phi_1(\tau)$ (solid red line) and the SH $\phi_2(\tau) = \frac{1}{4}\sigma P_1 \sin(|\tau|/\sigma)$ (dashed blue line). The close-up shows the oscillating tail of the FW.

of periodic solutions, where the imaginary part of ν is zero, while the real part increases abruptly.

Even though the solution in the full y space is unbounded, the solution can still be physical, given that $\tau > 0$ ($\tau < 0$) implies that only $y > -\pi/4$ ($y < -\pi/4$) is considered. Thus the physical solutions for $\tau > 0$ are those with a positive imaginary part of ν, for which the amplitude will decrease with y. This allows us to construct the physical bounded solutions to Eq. (12) as follows:

$$\Phi(\tau \geqslant 0) = c_1 F_\nu\left(a, q, \left[\frac{\tau}{2\sigma} - \frac{\pi}{4}\right]\right), \tag{15}$$

$$\Phi(\tau < 0) = c_2\, F_\nu\left(a, -q, -\left[\frac{\tau}{2\sigma} - \frac{\pi}{4}\right]\right). \tag{16}$$

From Eq. (12) we see that it is invariant to the transformation $(y,q) \to (\pm y \pm \pi/2, -q)$. This symmetry of MDE and thus its solutions $F_\nu(a,q,y)$ allow us to reduce the bounded solution further to either the symmetrical solution ($c_1 = c_2 = A_\nu e^{i\nu\pi/4}$)

$$\Phi^{\rm s}(\tau) = A_\nu\, e^{i\nu[\frac{|\tau|}{2\sigma}]} P\left(a, q, \frac{|\tau|}{2\sigma} - \frac{\pi}{4}\right) \tag{17}$$

or the antisymmetrical solution ($c_1 = -c_2 = A_\nu e^{i\nu\pi/4}$)

$$\Phi^{\rm as}(\tau) = {\rm sgn}(\tau)\, A_\nu\, e^{i\nu[\frac{|\tau|}{2\sigma}]} P\left(a, q, \frac{|\tau|}{2\sigma} - \frac{\pi}{4}\right). \tag{18}$$

Since MDE is a linear equation, we can redefine A_ν as a real parameter, which is then determined by the self-consistency relation $P_1 = A_\nu^2 \int_{-\infty}^{+\infty} [{\rm Re}\{\Phi(s)\}]^2 ds$. The function $P(a, \pm q, \pm y)$ is, as mentioned, π periodic in y. This means that it is periodic in τ with period $2\pi\sigma$.

The physical solution $\phi_1(\tau) = {\rm Re}\{\Phi(\tau)\}$ to the original equations (1) and (2) must be differentiable everywhere, including at $\tau = 0$. This is, in general, not the case for the solutions $\phi_1^{\rm s}(\tau)$ and $\phi_1^{\rm as}(\tau)$ defined in Eqs. (17) and (18), except for particular values of a and q, and thus σ and P_1, for which the solution goes through zero or has a local extremum at $\tau = 0$. This is nicely seen in Fig. 3, where the two lowest-power (i.e., the first and second) symmetric and antisymmetric solutions for $\sigma = 1$ are marked by widely separated green and black dots, respectively. In the following we analyze how the two types of solutions depend on the degree of nonlocality σ and the FW power P_1.

A. Validity of strongly nonlocal assumption

Before looking at the specific solutions, it is important to discuss when these physical MDE solutions will be accurate, i.e., when the approximation of strong nonlocality is valid. The $1/e$ width of the nonlocal response function $Q(\tau)$ is given by σ, and from analytical solutions (17) and (18) we see that the $1/e$ width of the envelope of the FW solution squared, $\phi_1^2(\tau)$, is $\sigma/{\rm Im}\{\nu\}$. The assumption of strong nonlocality implies that the response function is much broader than the function $\phi_1^2(\tau)$, which therefore means that ${\rm Im}\{\nu\} \gg 1$. From Fig. 3 we see that ${\rm Im}\{\nu\}$ is only around 1.5 for the lowest-power solutions for $\sigma = 1$, which means that the validity of the strongly nonlocal approximation is not as good for $\sigma = 1$. We will return to this point in the next section.

B. Antisymmetric solution

First, we consider the antisymmetric solutions of lowest power, which are soliton bound-state solutions with oscillating tails. Figure 4 shows the lowest-power antisymmetric solution for $\sigma = 1$, which has a power of $P_1 = 8.40$ (first black dot in Fig. 3). The FW peak separation is about 4, and in the close-up shown in Fig. 4 the rapidly decaying oscillations in the tails of the FW are visible.

It is important to emphasize that for any given σ we can find a solution, and thus we have a whole family of soliton bound-state solutions. Given that ${\rm Im}\{\nu\} = 1.44$ for the solution for $\sigma = 1$ shown in Fig. 4, it is not in the strongly nonlocal regime and therefore cannot be expected to be an accurate solution. To find the values of σ for which the solutions are in the strongly nonlocal regime, we plot in Fig. 5 the FW power P_1 and corresponding value of ${\rm Im}\{\nu\}$ and the peak separation for the family of antisymmetric soliton solutions with minimum P_1.

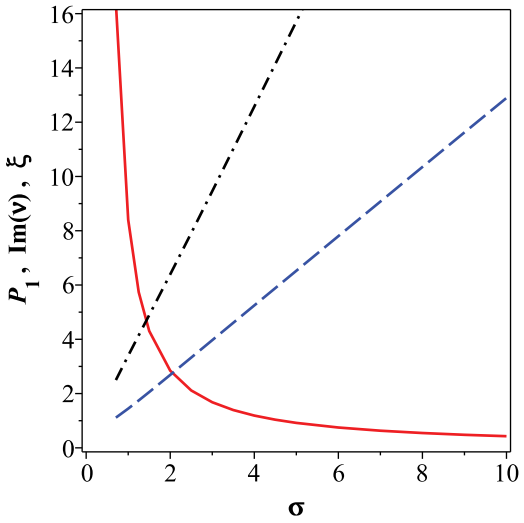

FIG. 5. (Color online) FW power P_1 (red solid line) and corresponding peak separation ξ (black dash-dotted line) and Im$\{\nu\}$ (blue dashed line) vs the degree of nonlocality σ for the antisymmetric soliton family with minimum P_1.

From Fig. 5 we see that σ should be larger than about 8 to be in the strongly nonlocal regime where Im$\{\nu\} > 10 \gg 1$, and we see that the soliton power P_1 decreases with σ. In Fig. 6 we therefore show the FW part of the lowest-power antisymmetric solution for $\sigma = 10$. The FW peak separation has now increased to about 32, and the solution looks like a bound state of two out-of-phase solitons. However, the FW still has oscillating tails even though they are not visible in Fig. 6. The power in the FW has now decreased to only $P_1 = 0.43$, but the imaginary part of the characteristic exponent has increased to Im$\{\nu\} = 12.89$, and thus this solution should actually be a good approximation of the exact soliton.

Continuous families of antisymmetric solutions as we find here have not been found analytically or numerically before. However, in the one special case of $\alpha = 2$, Buryak and Kivshar found the exact solution $\phi_1(\tau) = 6\sqrt{2}\tanh(\tau)\mathrm{sech}(\tau)$

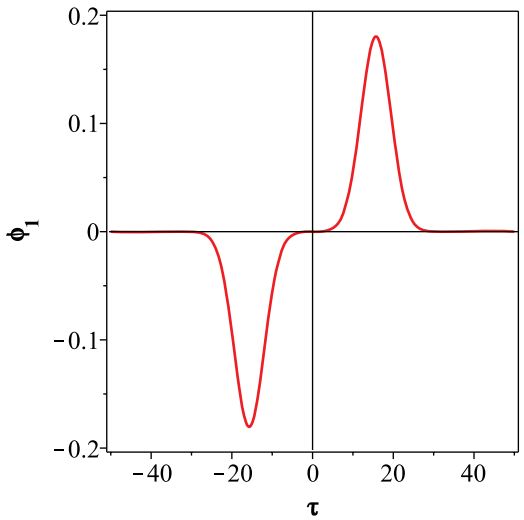

FIG. 6. (Color online) FW part $\phi_1(\tau)$ of the antisymmetric solution with lowest power $P_1 = 0.43$ ($\nu = 1 + i\,12.89$) for $\sigma = 10$.

and $\phi_2(\tau) = 6\mathrm{sech}^2(\tau)$ [10]. This solution can be used to test the accuracy of our solutions. This is illustrated in Fig. 7. A good agreement is not expected because $\alpha = 2$ corresponds to only $\sigma = 1/\sqrt{2}$. For the FW part we remarkably find that there is a quite good agreement with the exact solution anyway, with almost identical ($\Delta\tau = 2$) peak separation. In contrast the oscillatory strongly nonlocal SH solution is far from the exact localized solution.

A discrete set of similar antisymmetric soliton solutions was found exactly numerically in [10] for $s_1 = -s_2 = +1$ at discrete values of α between 12 and 50. Two examples showed FW solutions qualitatively similar to our solutions in Figs. 4 and 6, but the SH was localized. Unfortunately, these α values correspond to values of σ in a narrow region from 0.14 to 0.29, which is very far from the strongly nonlocal limit of $\sigma > 8$ in Fig. 5. Nevertheless, to compare with these solutions we plot in Fig. 8 the relative amplitude A_2/A_1 of the SH and FW solutions versus α, just as in Fig. 4 in [10].

The dependency of the relative amplitude of our continuous solution family on α (and thus σ) is qualitatively the same as that traced by the set of discrete points in [10]. In the limit $\alpha \to \infty$, corresponding to the weakly nonlocal NLS limit $\sigma \to 0$, one can neglect the second derivative in Eq. (2), and it is then easy to use the (single bright) NLS soliton solution to find (for $\alpha > 0$) that $A_2/A_1 \to 1/\sqrt{\alpha} = \sigma$. Whereas the relative amplitude of the solutions found in [10] also approach this limit, the relative amplitude of our solutions saturates around a value of 1 for $\alpha \gg 1$. Comparing Figs. 4–7 we further see that the width of the peaks and the peak separation both increase with the degree of nonlocality σ for our solution. In contrast, the numerical profile examples found in [10] show the exact opposite tendency, i.e., that the width and separation both decrease with σ.

One point to consider is that our solutions are only really valid for $\sigma > 8$, corresponding to $\alpha = 1/\sigma^2 < 0.016$, whereas the numerical solutions of [10] were only found for $\alpha > 12$. The two solutions therefore occupy completely different regimes in terms of the parameter α, which could be the reason for the opposite properties. It is worth noticing here that an investigation of bound states of out-of-phase nonlocal solitons for $s_2 = +1$ showed that the width of the individual solitons increases (as found here for $s_1 = -1$), while the separation decreases (like the Buryak and Kivshar solution for $s_2 = -1$) [38]. The discrepancy will be the subject of further investigation.

We finally note that since there seems to be a qualitative agreement between the shape of our FW solutions and the exact FW solutions (at least for $\alpha = 2$), then we could, in principle, find an improved SH solution $\phi_2^{\mathrm{im}}(\tau)$ by making an iteration and use the found FW solution in the convolution term,

$$\phi_2^{\mathrm{im}}(\tau) = \gamma \int_{-\infty}^{\infty} \phi_1^2(s) Q(\tau - s) ds = 0,$$

where $\gamma Q(\tau) = (\sigma/4)\sin(|\tau|/\sigma)$ in accordance with Eq. (8) for $s_2 = s_3 = -1$. In Fig. 9 we show the improved SH solution for $\alpha = 2$ together with the exact SH solution. As seen, the SH now peaks at $\tau = 0$ as we know it should. However, it is still oscillatory in nature, in contrast to the exact solution.

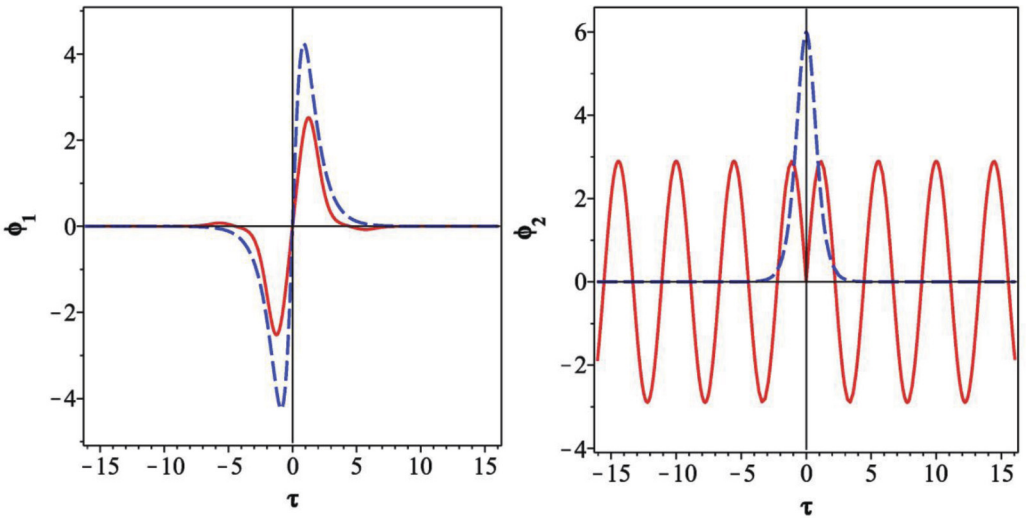

FIG. 7. (Color online) Comparison between our strongly nonlocal solution (solid red line) and the exact solution (dashed blue line) for (left) the FW $\phi_1(\tau) = 6\sqrt{2}\tanh(\tau)\mathrm{sech}(\tau)$ and (right) SH $\phi_2(\tau) = 6\mathrm{sech}^2(\tau)$ for $\alpha = 2$.

C. Symmetric solution

We now turn to the symmetric two-soliton bound-state solution, concentrating only on the solutions with lowest FW power P_1. These solutions, which have oscillating tails just as the antisymmetric solitons do, have never been found before. In Fig. 10 we show the FW part of the symmetric solution for $\sigma = 5$. The power in the FW is approximately 0.92, and the oscillating tails are there, even though they are not visible in Fig. 10.

Figure 11 shows the symmetric solutions for $\sigma = 2$, $\sigma = 1$, and $\sigma = 0.5$. The power in the FW is $P_1 \approx 2.75$, $P_1 \approx 6.69$, and $P_1 \approx 17.94$, respectively. As evident from Fig. 11 the separation between peaks decreases, and we go towards the single-peak soliton solution as σ decreases. However, as discussed above, it should be noted that for small values of σ the strongly nonlocal approach is not appropriate.

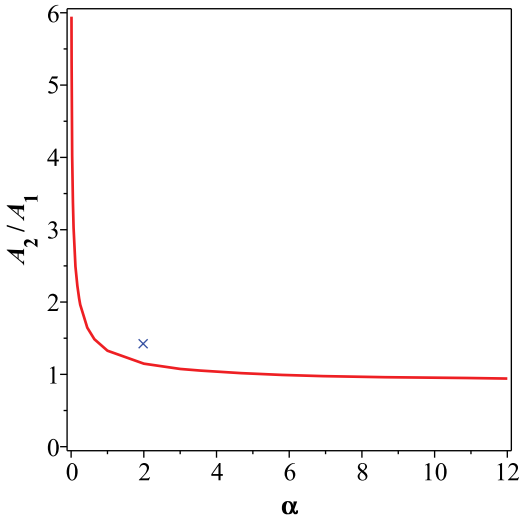

FIG. 8. (Color online) Relative amplitude A_2/A_1 of the antisymmetric SH and FW solutions of lowest power P_1 vs α. The blue cross indicates the value for the exact solution for $\alpha = 2$.

Again, we would like to emphasize that for any given value of σ we can find a solution, and thus we have a continuous family of symmetric in-phase soliton bound-state solutions. In Fig. 12 we plot the lowest value of P_1 and the corresponding value of the peak separation and imaginary part of ν as a function of σ for this family of solutions. When the nonlocality increases, the power of the FW decreases, and the peak separation increases, as seen in Fig. 5 for the family of antisymmetric soliton solutions, but the power is slightly lower for the symmetric solutions. From the imaginary part $\mathrm{Im}\{\nu\}$ we see that σ should again be larger than 8 in order for $\mathrm{Im}\{\nu\}$ to be larger than 10 and the solution to be in the strongly nonlocal regime.

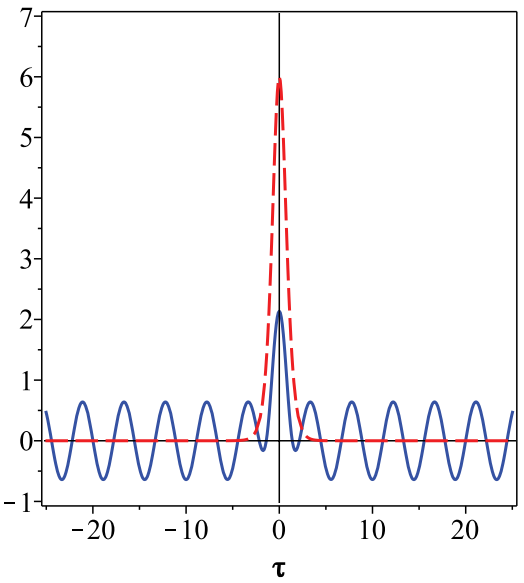

FIG. 9. (Color online) Exact analytical SH solution $\phi_2(\tau) = 6\mathrm{sech}^2(\tau)$ (red dashed line) and improved SH solution $\phi_2^{\mathrm{im}}(\tau)$ (blue solid line) for $\alpha = 2$ obtained by convolving the found FW solution with the response function.

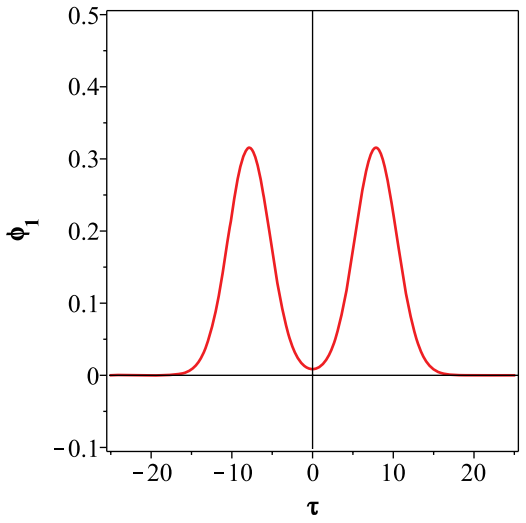

FIG. 10. (Color online) FW part $\phi_1(\tau)$ for the symmetric solution with the lowest FW power $P_1 \approx 0.92$ for $\sigma = 5$.

IV. NUMERICAL SIMULATION

From the work of Buryak and Kivshar [10] we know that all localized soliton solutions are unstable and radiate linear waves for $-s_1 = s_2 = -1$. Radiationless bound states of out-of-phase bright solitons were constructed by combining two such unstable solitons out of phase to eliminate the radiation on the outer side of the two solitons [10]. Numerically exact solutions were found to only exist for special *discrete* values of σ [10], which means that they were also unstable because any perturbation would release the radiation [10].

Here we have found continuous families of bound states of out-of-phase solitons and also in-phase solitons. However, due to the inherent instability of the individual solitons, the bound states should also still be unstable. To investigate the instability of our soliton families we have performed numerical

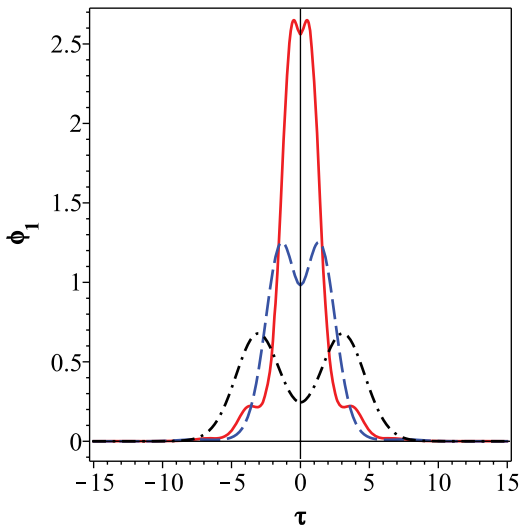

FIG. 11. (Color online) Symmetric solutions for $\sigma = 2$ (dash-dotted black line), $\sigma = 1$ (dashed blue line), and $\sigma = 0.5$ (solid red line). The power in the FW is $P_1 \approx 2.75$, $P_1 \approx 6.69$, and $P_1 \approx 17.94$, respectively. As σ is decreased we go towards the single-peak soliton solution.

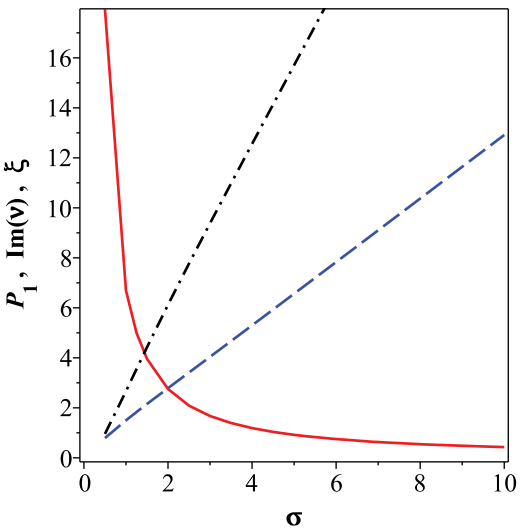

FIG. 12. (Color online) FW power P_1 (red solid line) and corresponding peak separation ξ (black dash-dotted line) and Im$\{\nu\}$ (blue dashed line) vs the degree of nonlocality σ for the symmetric soliton family with minimum P_1.

simulation and propagated our stationary solutions $\phi_{1,2}(\tau)$ in the original $\chi^{(2)}$ model [Eqs. (5) and (6)] for the normalized fields,

$$w(\xi,\zeta) = a_1\phi_1(\tau)e^{i\lambda\zeta}, \quad v(\xi,\zeta) = a_2\phi_2(\tau)e^{i2\lambda\zeta+i\beta\zeta},$$

using a split-step Fourier scheme with 2^{14} points in ξ and constant step size in ζ. We have fixed the parameters to $d_1 = -2d_2 = 2$ and $\lambda = -\beta = 2$, giving $s_1 = -s_2 = +1$, $a_1 = 1$, $a_2 = 2$, $\alpha = 2$, and $\tau = \xi$. In order to see the degree of instability inherent in the exact solutions we first propagate the exact analytical solution,

$$\phi_1(\tau) = 6\sqrt{2}\tanh(\tau)\mathrm{sech}(\tau), \quad \phi_2(\tau) = 6\mathrm{sech}^2(\tau),$$

which exists for $\alpha = 1/\sigma^2 = 2$.

The results of the simulation are shown in Fig. 13, from which we see that even the exact analytical solution is strongly unstable and breaks up after only six diffraction lengths, $L_D = \xi_0^2/(2|d_1|) = 0.81$, where $\xi_0 = \tau_0 = 1.8$ is the initial FWHM of the amplitude $\phi_1(\tau)$ of a single soliton in the FW bound state.

The instability observed for even the exact analytical solution implies that our approximate solution should be unstable and break up even before six diffraction lengths.

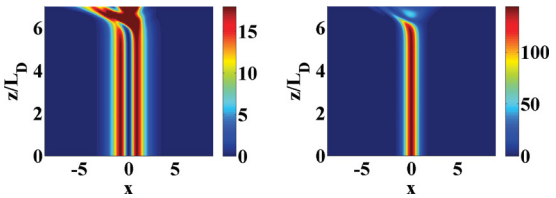

FIG. 13. (Color online) Evolution of exact analytical (left) FW and (right) SH soliton solution for $\alpha = 2$ in the original $\chi^{(2)}$ model [Eqs. (5) and (6)] over seven diffraction lengths, $L_D = \xi_0^2/(2|d_1|) = 0.81$, where $\xi_0 = 1.8$ is the initial FWHM of the FW amplitude. The simulation used $N_\xi = 2^{14}$ points in ξ with a resolution of $\Delta\xi = 2.4 \times 10^{-3}$ and $N_\zeta = 20\,000$ steps in ζ.

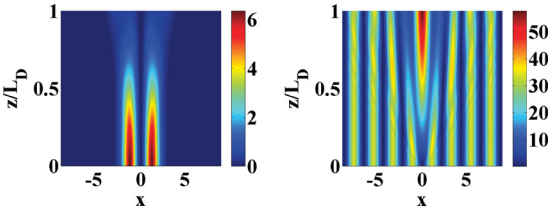

FIG. 14. (Color online) Evolution of approximate nonlocal (left) FW and (right) SH soliton solution for $\alpha = 2$ in the original $\chi^{(2)}$ model. Propagation is over one diffraction length, $L_D = \xi_0^2/(2|d_1|) = 0.72$, where $\xi_0 = 1.7$ is the initial FWHM of the FW amplitude. The simulation used $N_\xi = 2^{14}$ points in ξ with a resolution of $\Delta\xi = 1.9 \times 10^{-3}$ and $N_\zeta = 3000$ steps in ζ.

In Fig. 14 we show the corresponding evolution of our approximate solution, and we see that indeed the instability develops already after $L_D/2$. We have tested our approximate solutions for several other values of σ and found that they are indeed all unstable in propagation.

In a sense this is not surprising. We already mentioned that our highly nonlocal approximation is rather crude. It relies on replacing the convolution integral Eq. (8) by the product of the nonlocal response function and the intensity of the fundamental beam. While this leads to a rather reasonable solution for the fundamental beam, it fails to correctly represent the second harmonic. By virtue of our nonlocal approximation the second harmonic is periodic and delocalized, which is, strictly speaking, incorrect. As we already mentioned the approximation can be improved by using the calculated intensity profile of the fundamental wave to evaluate the correction to the amplitude of the second harmonic via the convolution integral (see Fig. 9). However, even in this case we found the solutions to be unstable in propagation, and this is indicative of the general stability of these quadratic solutions existing for $s_1 = -s_2 = +1$.

V. CONCLUSIONS

We have used the formal analogy between quadratic and nonlocal solitons to study the soliton formation in quadratic media in the regime of negative diffraction of the second harmonic. We employed the highly nonlocal limit to transfer the original system of coupled equation for the FW and its SH into a linear Schrödinger-type equation with periodic potential. In this approximation, the formation of solitons is equivalent to localized defect states of this periodic potential.

We found continuous families of bound-state solutions of both in-phase and out-of-phase bright quadratic solitons and analyzed these in terms of their dependence on the degree of nonlocality σ, which is related to the nonlinearity parameter α as $\sigma = 1/\sqrt{|\alpha|}$. For both families the power decreased and the separation increased as the degree of nonlocality increased, which means that the bound state tends towards two widely separated weak solitons coupled by a strongly nonlocal nonlinearity. For both families we found that the assumption of strong nonlocality required $\sigma > 8$.

The family of in-phase solitons has not been found before, but our family of out-of-phase solitons can be compared with an exact analytical solution for $\alpha = 2$ and a discrete set of exact out-of-phase solitons found numerically by Buryak and Kivshar [10]. Even though our SH is by nature periodic, our FW compares nicely to the exact analytical solution. We have found the relation between the relative SH and FW amplitude (A_2/A_1) and the nonlinearity parameter α and found it to decay as the exact numerical solution but saturate towards 1 and not 0 [10]. We have also found that the dependence of the peak separation and the width of the peaks on the nonlinearity parameter is opposite to the numerically found solution and argued that this could be due to the fact that our nonlocal solutions are accurate in the strongly nonlocal limit of $\sigma > 8$, corresponding to $\alpha < 0.016$, while the numerical solutions have only been found for a discrete set of values of α above 12.

Our nonlocal approach provides families of solutions and physical insight into the properties of soliton formation in quadratic media in the regime of negative diffraction of the second harmonic. We note that, in fact, in general, nonlocal systems, using the strongly nonlocal approach, are well known to provide physical insight and good approximate solutions [16,19,39–46]. However, this has not been applied to a nonlocalized periodic response function before.

ACKNOWLEDGMENTS

M.B. acknowledges the Danish Council for Independent Research Projects 274-08-0479 and 11-106702.

[1] G. Stegeman, D. J. Hagan, and L. Torner, Opt. Quantum Electron. **28**, 1691 (1996).
[2] A. V. Buryak, P. Di Trapani, D. V. Skryabin, and S. Trillo, Phys. Rep. **370**, 63 (2002).
[3] M. M. Fejer, G. A. Magel, D. H. Jundt, and R. L. Byer, IEEE J. Quantum Electron. **28**, 2631 (1992).
[4] A. Kobyakov, F. Lederer, O. Bang, and Yu. S. Kivshar, Opt. Lett. **23**, 506 (1998).
[5] O. Bang, T. W. Graversen, and J. F. Corney, Opt. Lett. **26**, 1007 (2001).
[6] J. F. Corney and O. Bang, Phys. Rev. E **64**, 047601 (2001).
[7] C. B. Clausen, O. Bang, and Yu. S. Kivshar, Phys. Rev. Lett. **78**, 4749 (1997).
[8] S. K. Johansen, S. Carrasco, L. Torner, and O. Bang, Opt. Commun. **203**, 393 (2002).
[9] C. B. Clausen, Yu. S. Kivshar, O. Bang, and P. L. Christiansen, Phys. Rev. Lett. **83**, 4740 (1999).
[10] A. V. Buryak and Yu. S. Kivshar, Phys. Lett. A **197**, 407 (1995).
[11] Yu. N. Karamzin and A. P. Sukhorukov, JETP Lett. **20**, 339 (1974) [Sov. Phys. JETP **41**, 414 (1976)].
[12] V. V. Steblina, Yu. S. Kivshar, M. Lisak, B. A. Malomed, Opt. Commun. **118**, 345 (1995).
[13] A. A. Sukhorukov, Phys. Rev. E **61**, 4530 (2000).
[14] L. Berge, O. Bang, J. J. Rasmussen, and V. K. Mezentsev, Phys. Rev. E **55**, 3555 (1997).
[15] G. Assanto and G. I. Stegeman, Opt. Express **10**, 388 (2002).

[16] W. Krolikowski, O. Bang, N. I. Nikolov, D. Neshev, J. Wyller, J. J. Rasmussen, and D. Edmundson, J. Opt. B **6**, S288 (2004).
[17] I. V. Shadrivov and A. A. Zharov, J. Opt. Soc. Am. B **19**, 596 (2002).
[18] C. Conti, M. Peccianti, and G. Assanto, Phys. Rev. Lett. **91**, 073901 (2003).
[19] N. I. Nikolov, D. Neshev, O. Bang, and W. Z. Krolikowski, Phys. Rev. E **68**, 036614 (2003).
[20] S. K. Turitsyn, Teor. Mat. Fiz. **64**, 226 (1985).
[21] O. Bang, W. Krolikowski, J. Wyller, and J. J. Rasmussen, Phys. Rev. E **66**, 046619 (2002).
[22] O. Bang, D. Edmundson, and W. Krolikowski, Phys. Rev. Lett. **83**, 5479 (1999).
[23] W. Krolikowski, O. Bang, and J. Wyller, Phys. Rev. E **70**, 036617 (2004).
[24] O. Bang, P. L. Christiansen, F. If, K. Ø. Rasmussen, and Yu. B. Gaididei, Phys. Rev. E **49**, 4627 (1994).
[25] M. Bache, O. Bang, J. Moses, and F. W. Wise, Opt. Lett. **32**, 2490 (2007).
[26] M. Bache, O. Bang, W. Krolikowski, J. Moses, and F. W. Wise, Opt. Express **16**, 3273 (2008).
[27] P. V. Larsen, M. P. Sørensen, O. Bang, W. Z. Krolikowski, and S. Trillo, Phys. Rev. E **73**, 036614 (2006).
[28] J. Wyller, W. Krolikowski, O. Bang, D. E. Petersen, and J. J. Rasmussen, Phys. D **227**, 8 (2007).
[29] M. Abramowitz and I. A. Stegun, *Handbook of Mathematical Functions* (Dover, New York, 1972).
[30] C. R. Menyuk, R. Schiek, and L. Torner, J. Opt. Soc. Am. B **11**, 2434 (1994).
[31] O. Bang, J. Opt. Soc. Am. B **14**, 51 (1997).
[32] W. Z. Krolikowski and O. Bang, Phys. Rev. E **63**, 016610 (2000).
[33] E. M. Conwell, Appl. Phys. Lett. **23**, 328 (1973).
[34] W. Paul, Rev. Mod. Phys. **62**, 531 (1990).
[35] O. Morsch and M. Oberthaler, Rev. Mod. Phys. **78**, 179 (2006).
[36] P. Russell, Appl. Phys. B **39**, 231 (1986).
[37] J. D. Joannopoulos, R. D. Meade, and J. N. Winn, *Photonic Crystals: Molding the Flow of Light* (Princeton University Press, Princeton, NJ, 1995).
[38] P. D. Rasmussen, O. Bang, and W. Z. Krolikowski, Phys. Rev. E **72**, 066611 (2005).
[39] D. Deng, X. Zhao, Q. Guo, and S. Lan, J. Opt. Soc. Am. B **24**, 2537 (2007).
[40] D. Deng, Q. Guo, and W. Hu, Phys. Rev. A **79**, 023803 (2009).
[41] W.-P. Zhong and M. Belic, Phys. Rev. A **79**, 023804 (2009).
[42] C. Conti, M. A. Schmidt, P. St. J. Russell, and F. Biancalana, Phys. Rev. Lett. **105**, 263902 (2010).
[43] W.-P. Zhong, M. Belic, T. W. Huang, and R. H. Xie, Eur. Phys. J. D **59**, 301 (2010).
[44] J.-Y. Zhao, Q. Wang, M. Shen, J.-L. Shi, Q. Kong, and L.-J. Ge, Chin. Phys. B **19**, 054211 (2010).
[45] D. Deng and Q. Guo, Opt. Commun. **283**, 3777 (2010).
[46] Z. Yang, D. Lu, D. Deng, S. Li, W. Hu, and Q. Guo, Opt. Commun. **283**, 595 (2010).